

# Relaxation Oscillations of the Synchrotron Motion Caused by Narrow-Band Impedance

J. Sebek, C.Limborg  
SSRL/SLAC

# 1 Outline

- SPEAR parameters
- Motivations
- Experimental data to characterize phenomenon
  - Spectrum analyzer
  - Streak camera
- Simulations to increase understanding
- Analytical model that explains this behavior

## 2 SPEAR Parameters

3 GeV  $e^-$  storage ring dedicated to synchrotron radiation

- ultra-relativistic ( $\beta \cong 1$ )  $\Rightarrow$  no transition
- space charge effects negligible
- significant synchrotron radiation and associated damping

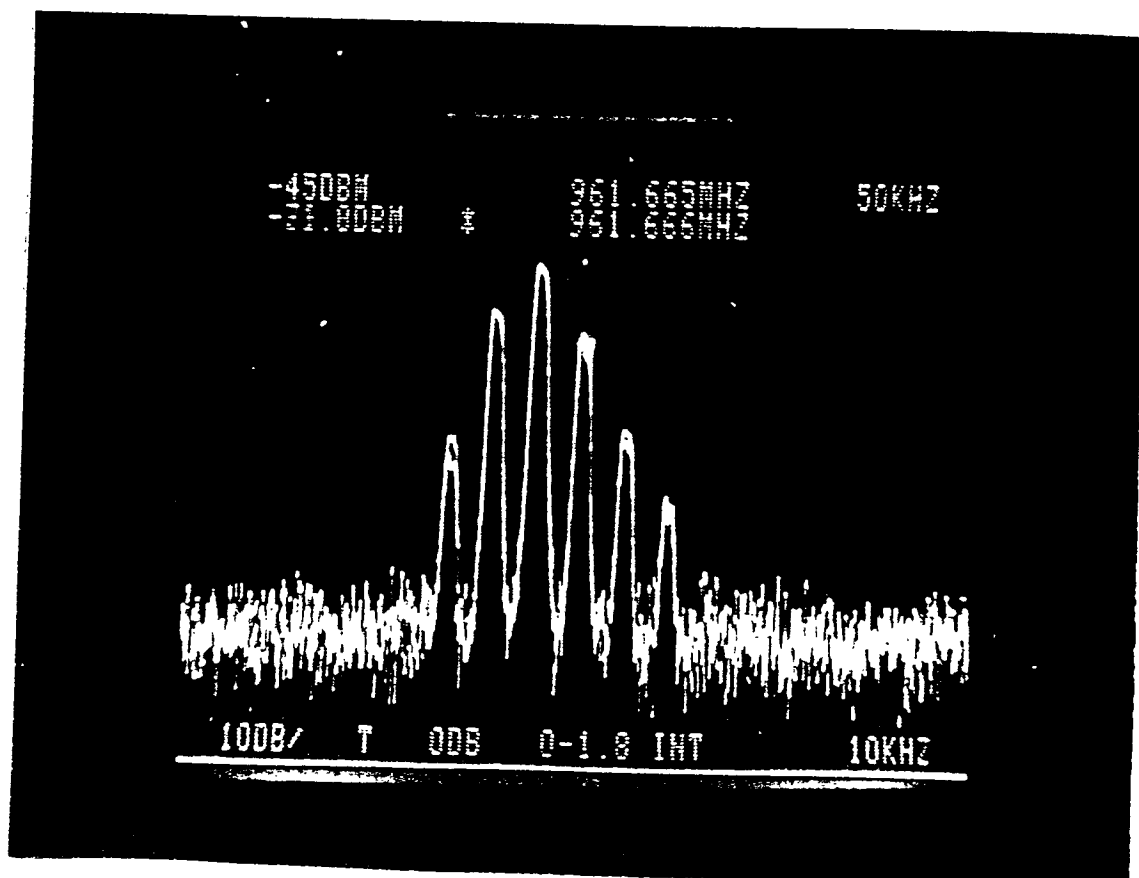
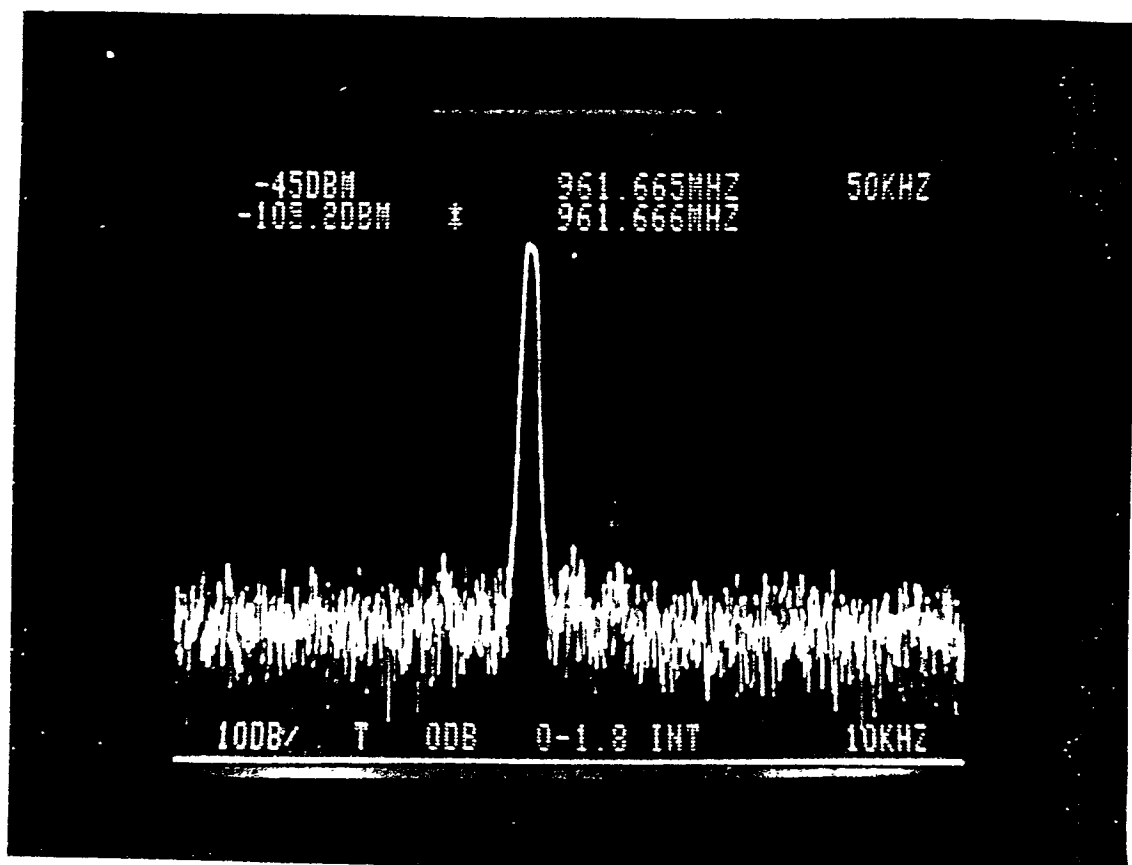
<b>Energy</b>	<b>2.3 GeV</b>	<b><u>HOM studied</u> = Fundamental</b>	
<b>Natural Damping Time</b>	<b>10 ms</b>	<b><math>f_{res} = f_{rf} = 358.533 \text{ MHz}</math></b>	
<b>Measured Damping Time</b>	<b>5 ms (@2mA)</b>	<b><math>R_s = 10 \text{ M}\Omega</math></b>	
<b>Bunch spectrum (<math>\sigma_r^{-1}</math>)</b>	<b>2.8 GHz</b>	<b>57 ps</b>	<b>1/49 RF bucket</b>
$f_{rf} = f_{HOM}$	<b>358.533 MHz</b>	<b>2.8 ns</b>	<b>1/280 turn</b>
$f_o$	<b>1.28 MHz</b>	<b>0.78 <math>\mu\text{s}</math></b>	<b>1 turn</b>
<b>Damping of HOM resonance</b>	<b>56 kHz</b>	<b>17.8 <math>\mu\text{s}</math></b>	<b>23 turns</b>
$f_{so}$	<b>28.4 kHz</b>	<b>35 <math>\mu\text{s}</math></b>	<b>45 turns</b>
<b>Relaxation oscillation</b>	<b>&lt;100 Hz</b>	<b>&gt;10 ms</b>	<b>&gt;12800 turns</b>

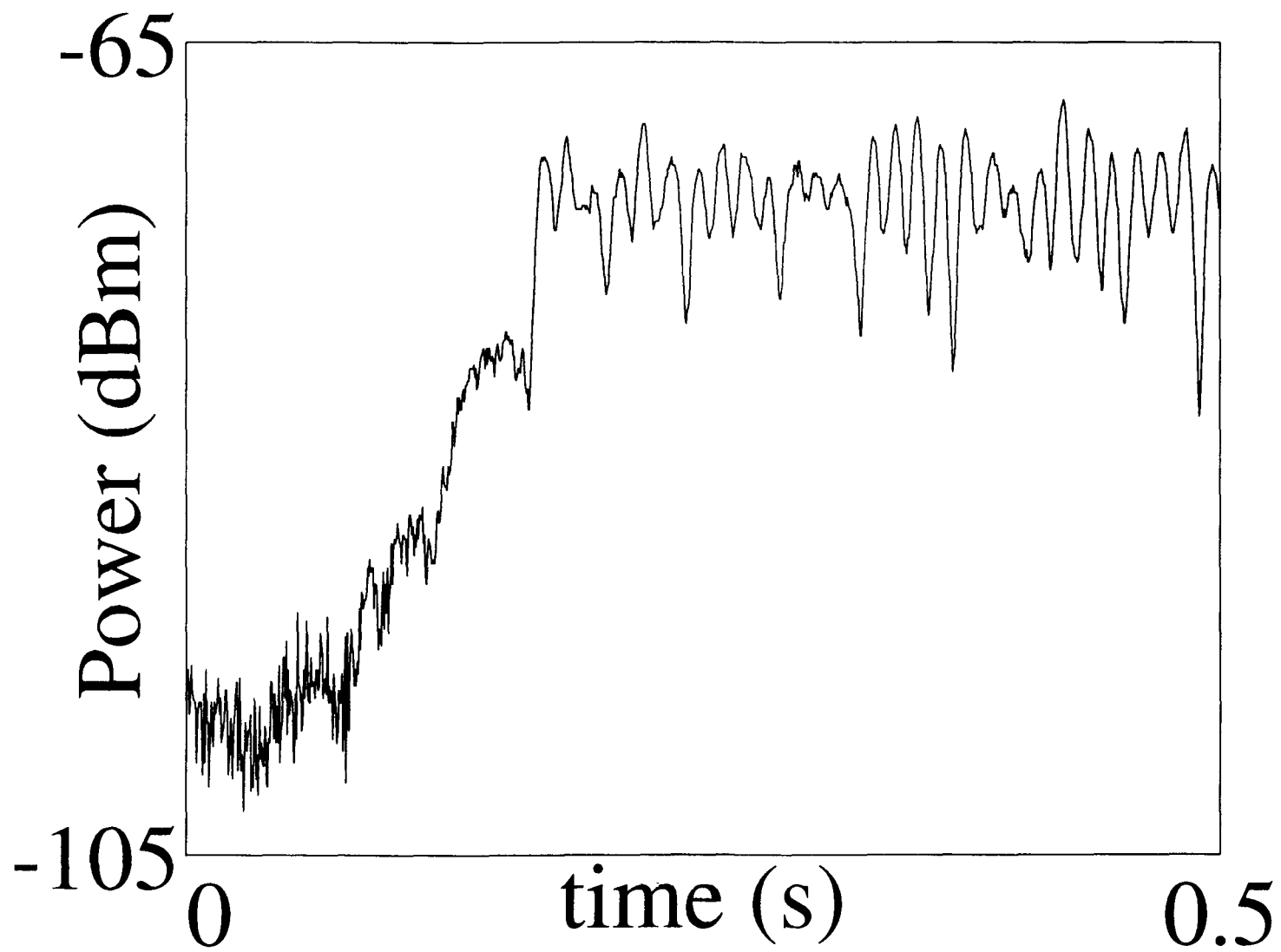
### 3 Motivation

- SPEAR has two 5-cell PEP-III/LEP style RF cavities
  - One cavity active, one cavity passive in normal operation
  - Two moveable tuners in each 5-cell cavity
- Work done to improve stability of operating point with respect to cavity HOMs
  - No HOM dampers on cavities
  - No longitudinal or transverse feedback systems
  - No temperature regulation on cavities
- Characterized HOMs vs tuner position

## 4 Observations

- Longitudinal oscillations saturate
- Envelope, itself, oscillates at very low frequency (three orders of magnitude smaller than  $\omega_s$ )
- Previously experimentally observed and reported
  - PhotonFactory [Yamazaki 1983]
  - Surf 2 [Rakowsky 1985]
  - Elettra [Wrulich 1996]
- Previously studied theoretically
  - Suzuki and Yokoya [1982]
  - Krinsky [1985]
  - Nagaoka [1996]
- Characterized this behavior on largest impedance available, the fundamental mode of the idle cavity, using signals from a pickup within the cavity





## 5 Spectrum Analyzer Results

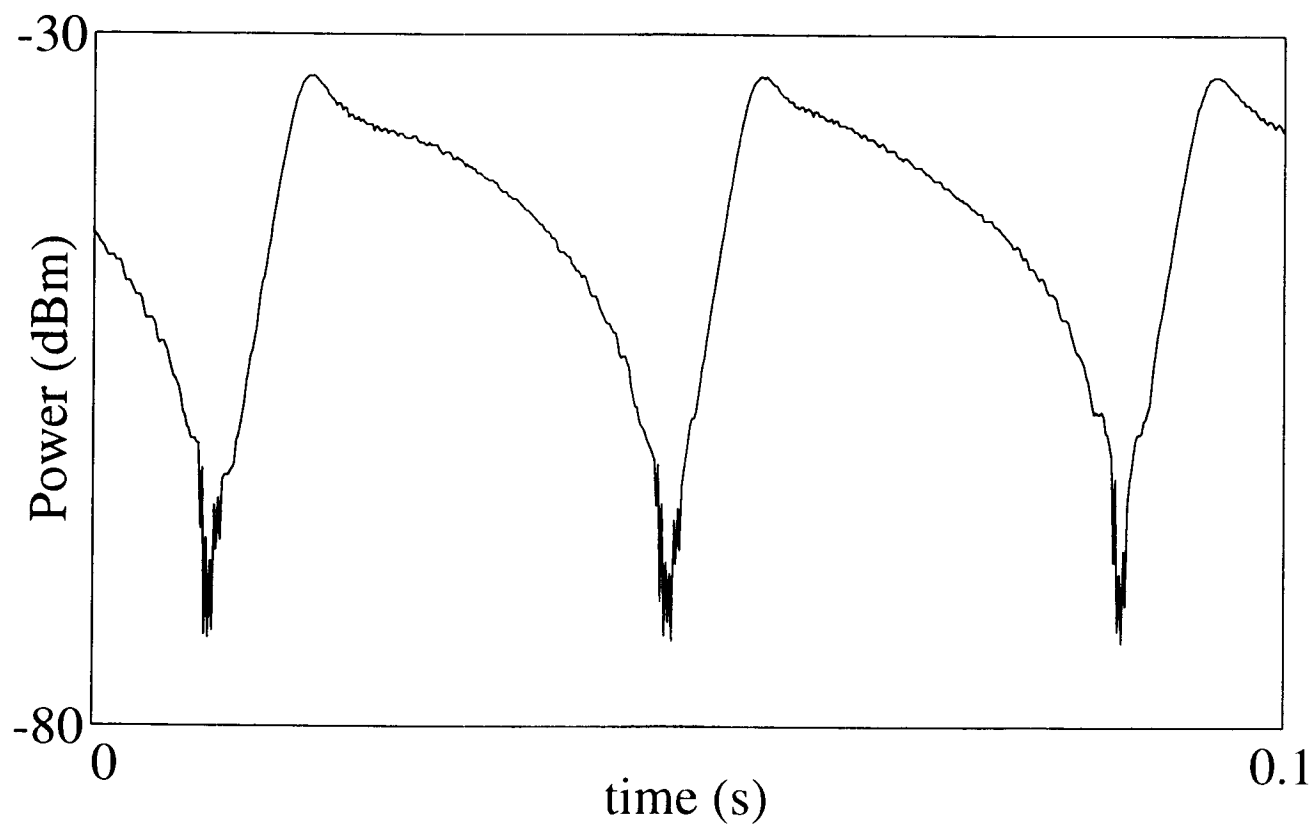
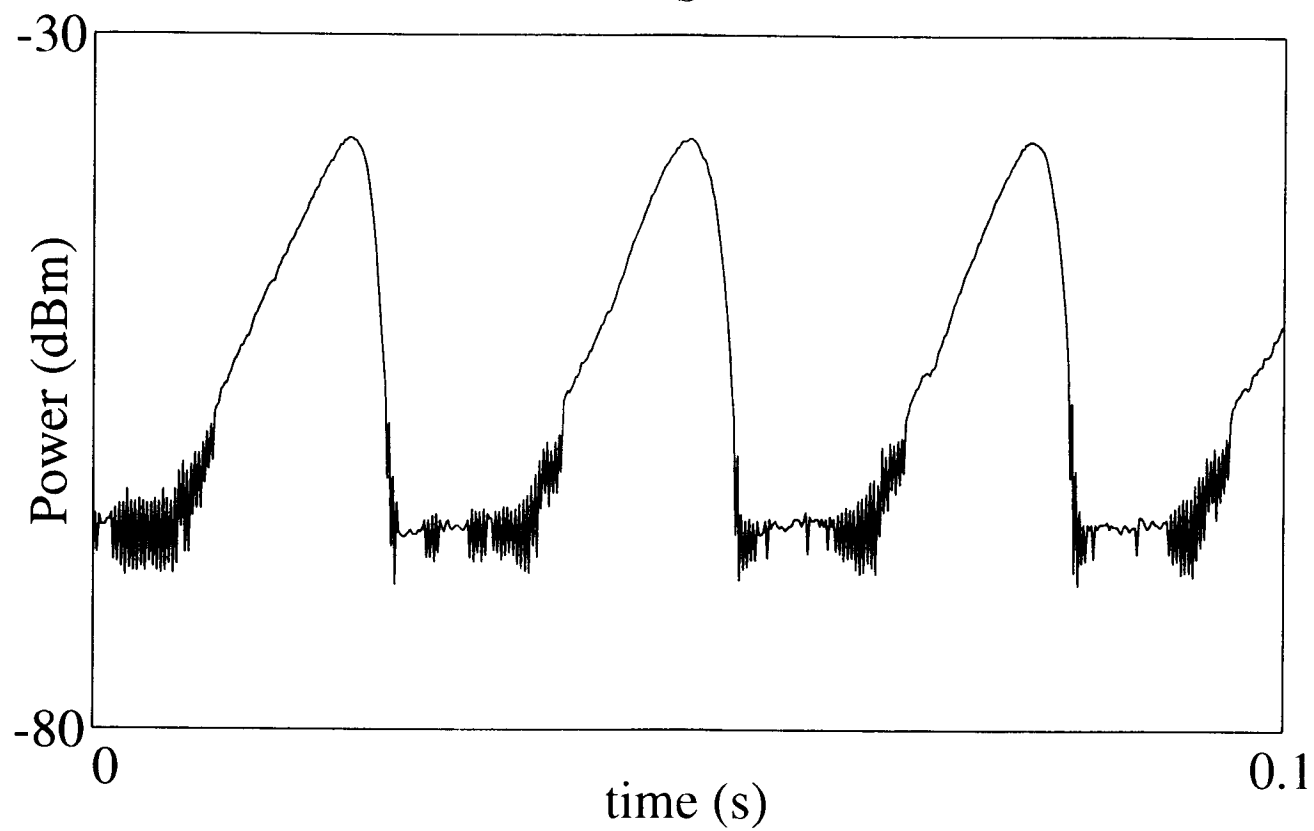
- Low oscillation frequency  $< 100$  Hz ( $\sim \tau_{\text{radiation damping}}^{-1}$ )
- Extends almost over entire region of instability
- Symmetry of growth time follows  $R(\omega_{HOM}) = R(p\omega_0 + \omega_z)$
- Asymmetry of damping
  - Complex damping mechanism
  - Explains frequency asymmetry
- Broadening of synchrotron frequency line:
  - $\Delta f_s \sim -15\%$

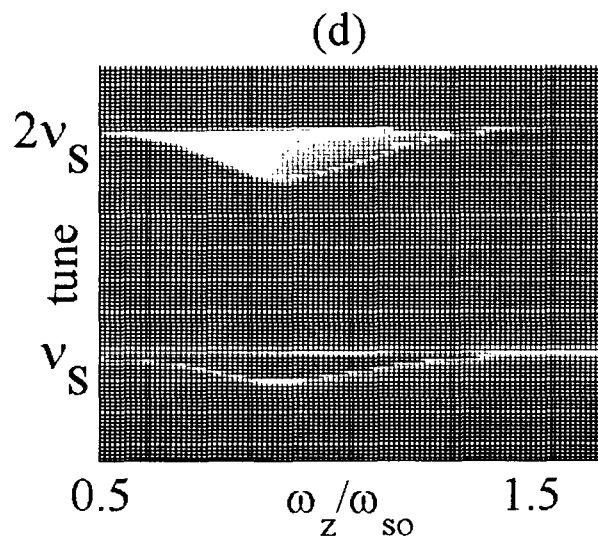
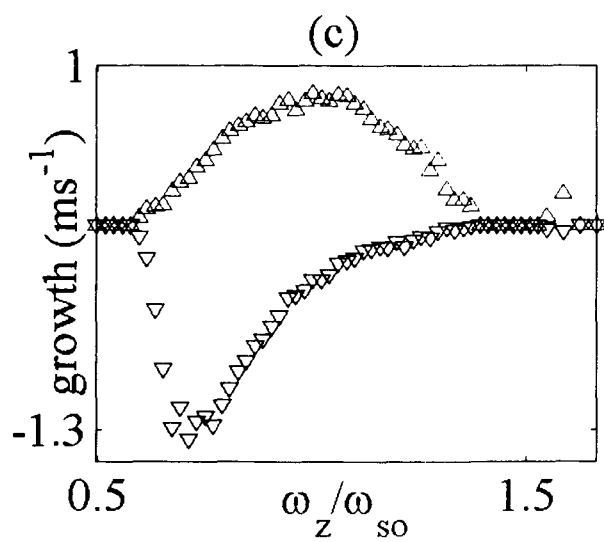
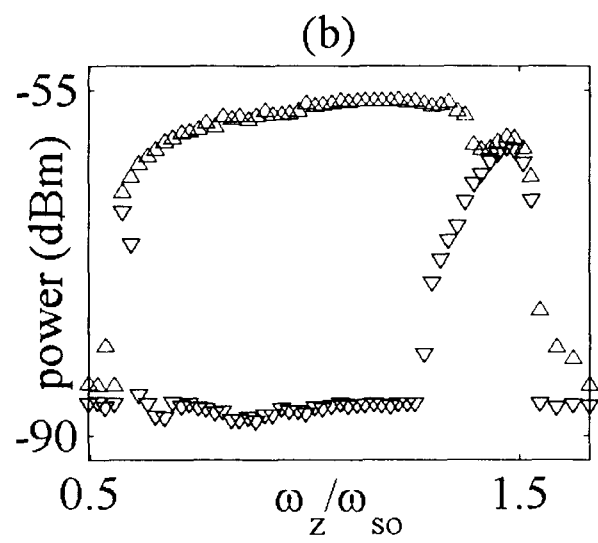
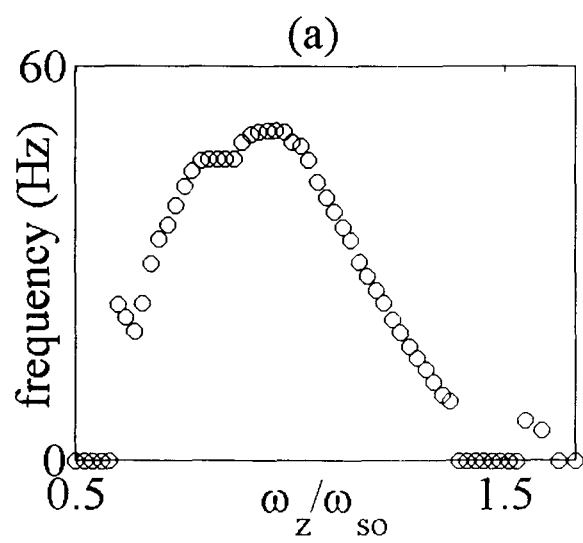
The oscillation amplitude initially grows toward an attractor at  $\infty$ . Then the dynamics of the system change so that the motion evolves toward another attractor. We call this cycle a **relaxation oscillation**.

These data give information only about the dipole moment of the bunch. We want to see its internal structure as well



power of upper  $v_s$  sideband vs time



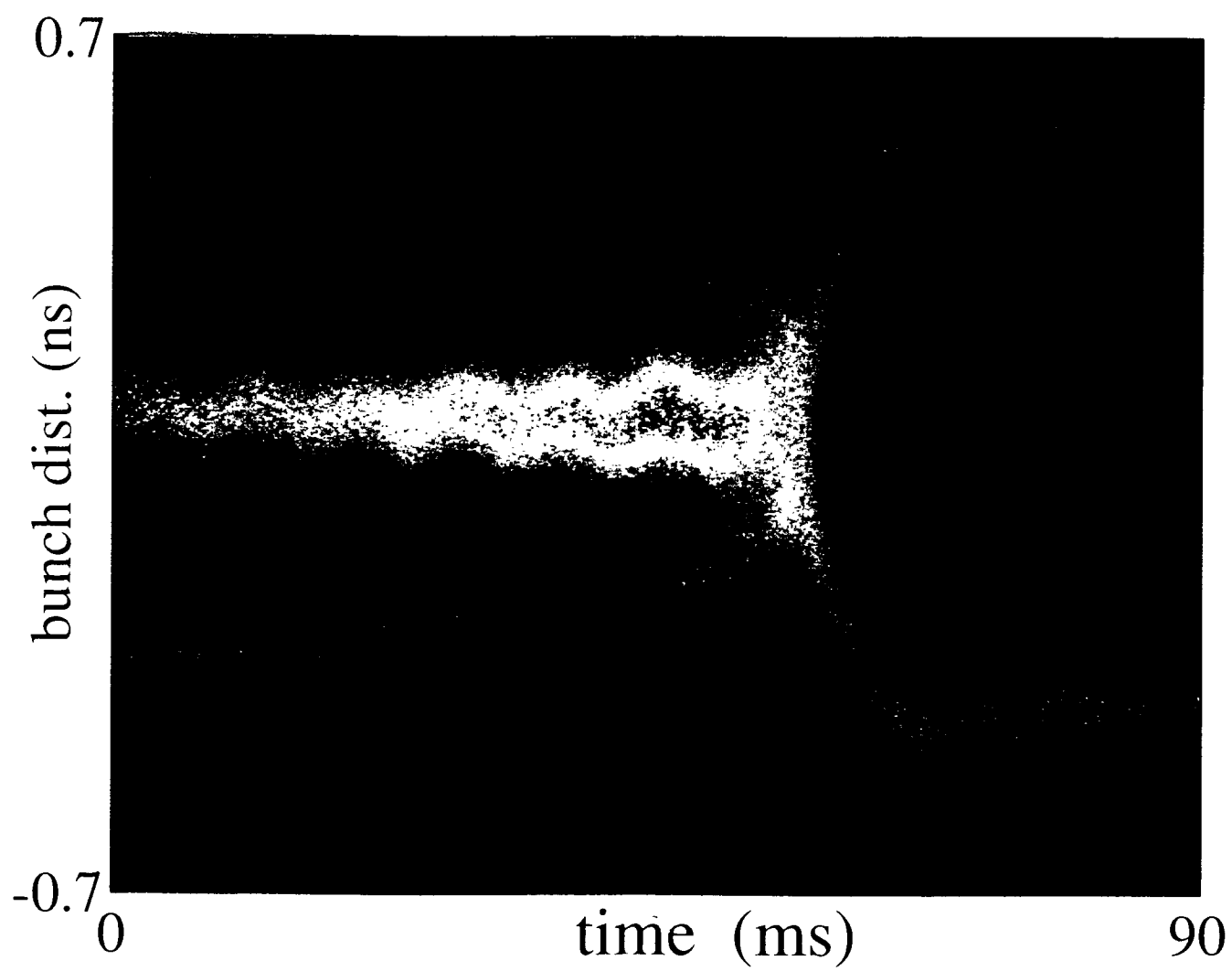


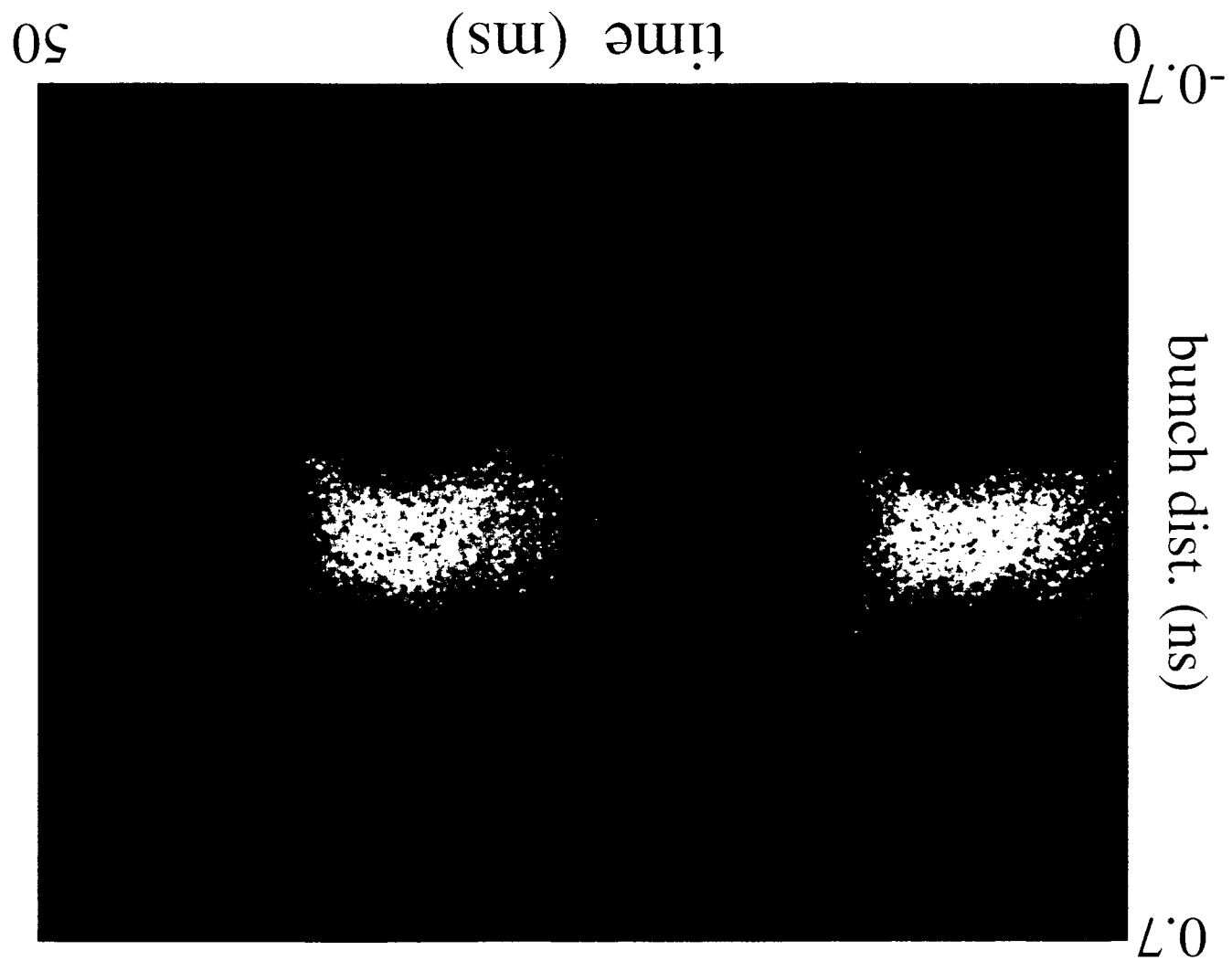
## 6 Streak Camera

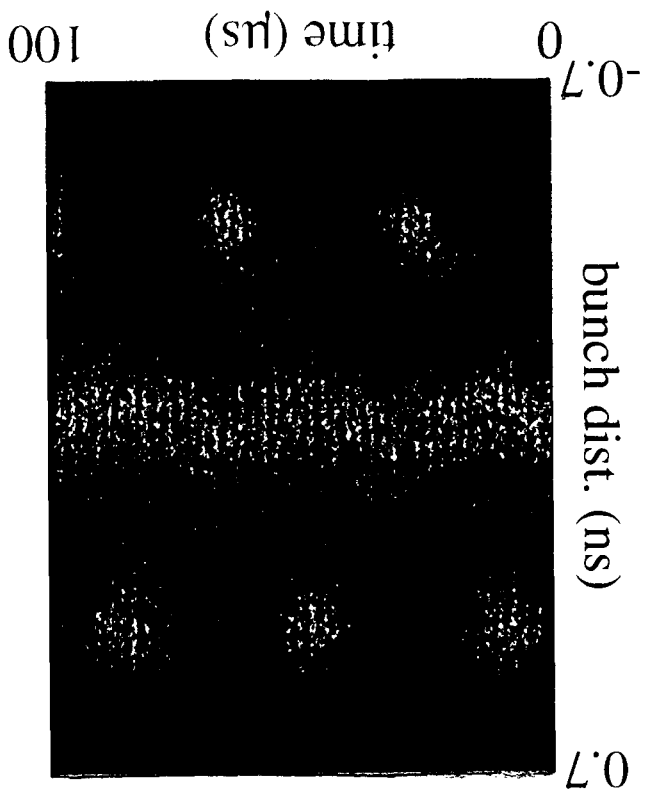
- Since the bunch is too short to examine its time distribution electronically, we used a streak camera to optically view this dimension.
- We were assisted by colleagues J. Hinkson and J. Byrd (LBNL), A. Fisher (SLAC) and A. Lumpkin (APS) in obtaining the beautiful pictures
- Dual sweep streak camera
  - Synchrotron radiation emitted by bunch is image of longitudinal  $e^-$  distribution
  - Camera converts  $\gamma$ 's to  $e^-$ 's in camera photocathode
  - Rotates longitudinal distribution of  $e^-$  to vertical distribution
  - Sweeps slowly in horizontal direction to image different bunches
  - Shows bunch envelope over long times on slow sweeps
  - Synchronized with  $f_{RF}$ , it shows bunch by bunch distributions on fast sweeps

## 7 Results from Streak Camera Images

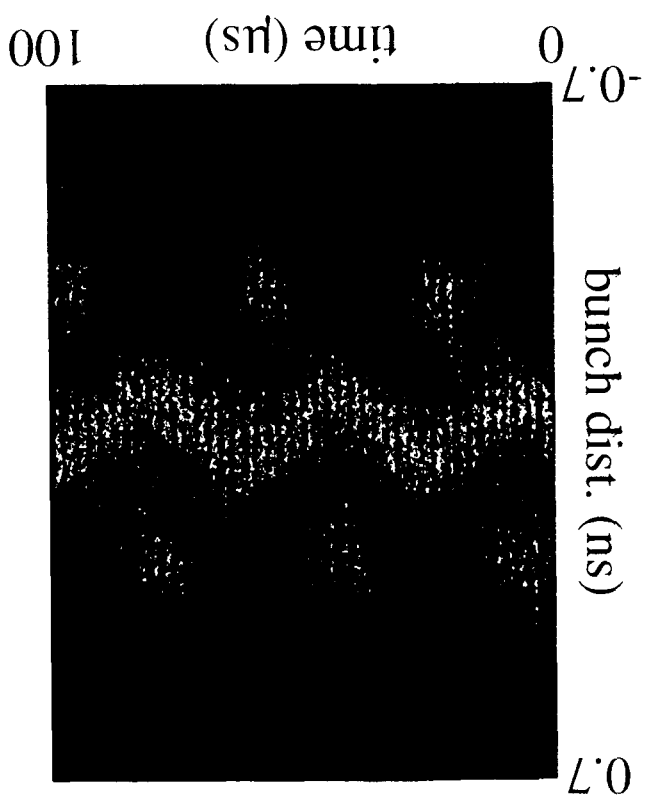
- Correlates, as expected, with data from spectrum analyzer
- Stays confined as a single macroparticle in initial phase of relaxation cycle
- Loss of intensity during growth
  - Particles start to escape from the bunch and are seen distributed over time
- Large amplitude of oscillations ( $\pm\pi/2$ ) i.e. 1/2 RF bucket size
  - Pendulum frequency decreases quadratically with amplitude
  - Spectrum analyzer data showed this 15% frequency shift over the relaxation cycle
- Attractor at finite amplitude
- In most cases, images show bunch collapses to center and begins new cycle
- In the particular case of  $\omega_z > \omega_s$  and a very slow damping rate, a 2<sup>nd</sup> attractor appears at the center
  - $\sim \pi$  out of phase with main body (or ‘initial attractor’)
  - starts growing while the ‘initial attractor’ is still damping



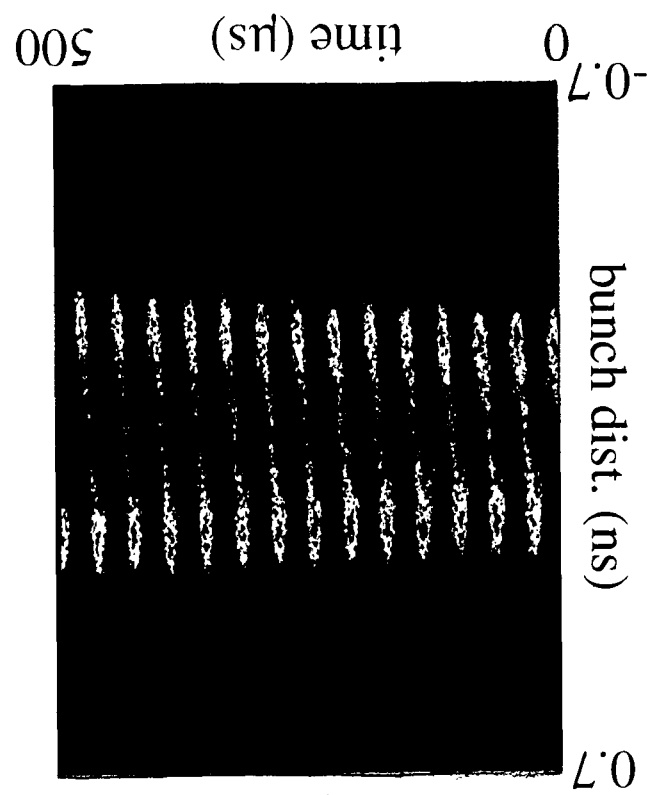




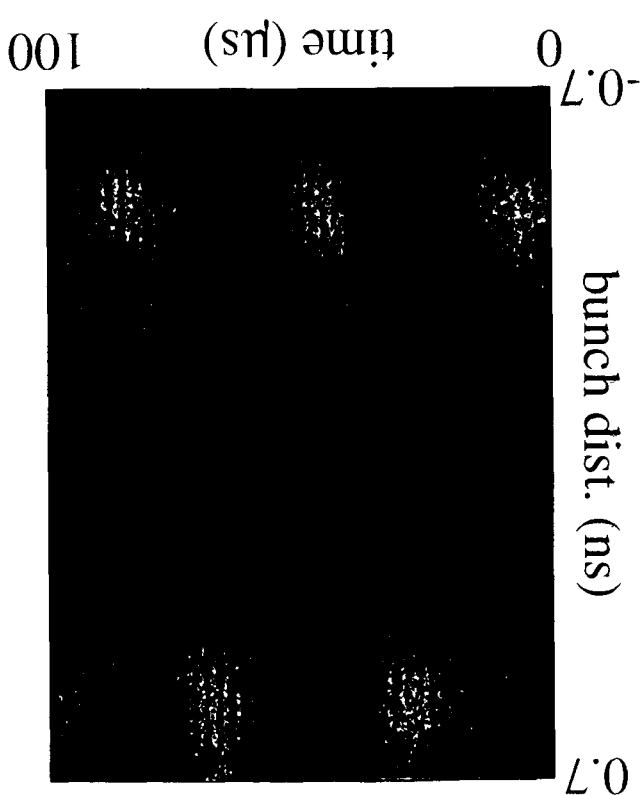
(c)



(d)



(a)



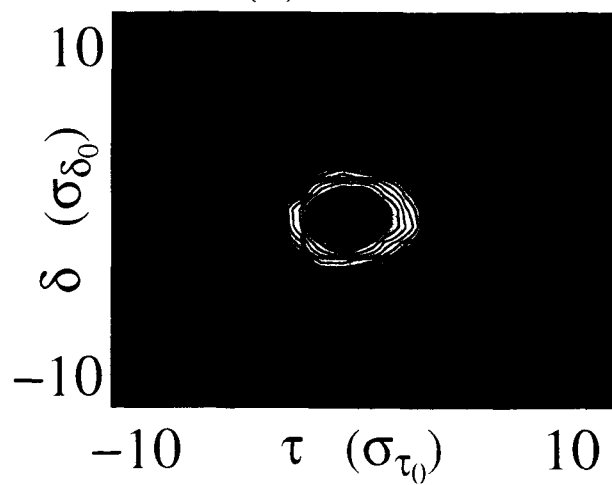
(b)

## 8 Simulations

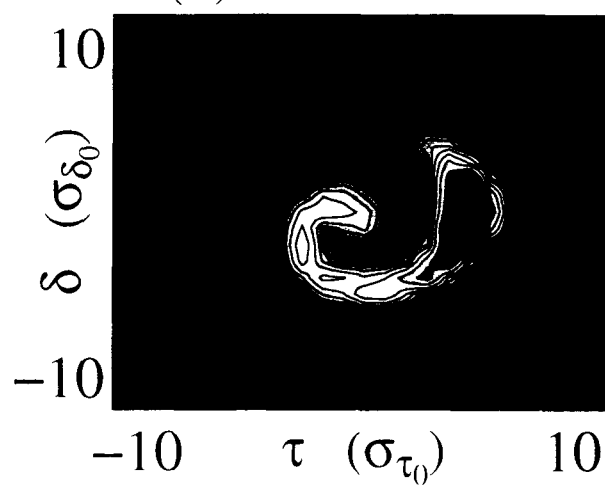
- Photon intensity from optical port too low to get all the information desired from longitudinal distribution.
- Used a multiparticle tracking code to get more information about the behavior of the relaxation oscillation.
- Implements the standard synchrotron equations of motion, including quantum fluctuations and wake function.
- The long range wake is calculated from turn to turn using propagators.
- The code reproduced well the main behavior:
  - Instability thresholds
  - Relaxation oscillation and its frequency
  - Diffusion from bunch
- Predictions from simulations
  - Diffusion is from the front of the bunch
  - Particles spiral toward the center of the bunch to restart cycle



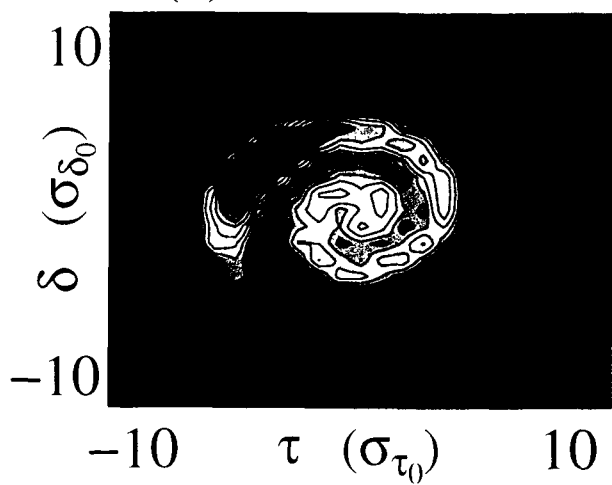
(a)  $t = 0$  ms



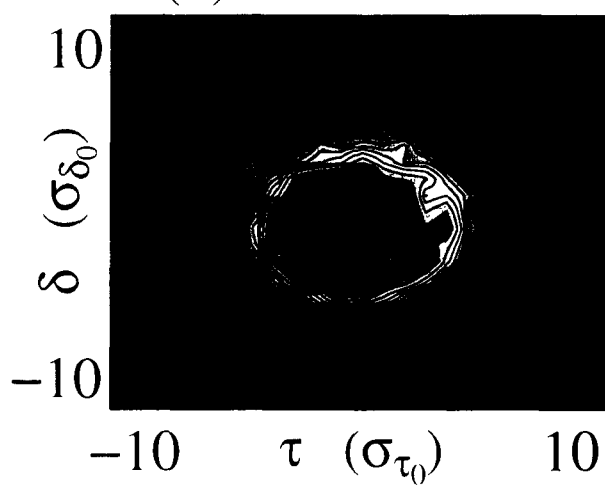
(b)  $t = 7.84$  ms



(c)  $t = 9.36$  ms



(d)  $t = 15.6$  ms



## 9 Analytical Model

### 9.1 Goals

Based on the experimental data and computer simulations, we would like the analytical model to explain:

- Instability thresholds given by linear theory
- Saturation mechanism of oscillation
- Diffusion, from the head of the bunch, as the amplitude grows
- Conditions for relaxation oscillation
  - Formation of second attractor
  - Damping mechanism
- For  $\omega_z > \omega_s$ , behavior of second attractor
  - $\sim \pi$  out of phase with initial attractor
  - growth as initial attractor damps

## 9.2 Driving Term – Wake•eld

Our goal is to express the driving term of this oscillation, the wake•eld, in a closed, analytical form that can be exploited for calculations. We use the experimental data and vastly different time scales of the system to justify the following simplifying approximations:

- $(\sigma_\tau \ll 2\pi/\omega_R) \Rightarrow$  use impulse approximation for single pass of wake•eld ( $Q \gg 1$ )  
 $V(t-u) = NeW(t-u) = NeU(t-u) 2\alpha_R R_{Se}^{-\alpha_R(t-u)} \cos \omega_R(t-u)$
- (cavity length  $\ll$  ring circumference)  $\Rightarrow$  total wake is in•nite summation

$$V(t) = 2\alpha_R R_S (Ne) \sum_{k=-\infty}^n e^{-\alpha_R(t(nT_0)-u(kT_0))} \cos \omega_R(t(nT_0)-u(kT_0))$$

- $(\alpha_R \ll f_0) \Rightarrow$  approximate summation with integral

$$V(t) = 2\alpha_R R_S \left( \frac{Ne}{T_0} \right) \int_{-\infty}^t e^{-\alpha_R(t-u)} \cos \omega_R(t-u) du$$

- $t = nT_0 + \tau_t, u = kT_0 + \tau_u, \omega_R = p\omega_0 + \omega_z \Rightarrow$  remove multiples of  $2\pi$  from cos

$$V(t) \cong 2\alpha_R R_S I \int_{-\infty}^t e^{-\alpha_R(t-u)} \cos [\omega_R(\tau_t - \tau_u) + \omega_z(t-u)] du$$

- instantaneously, motion always closely approximates harmonic oscillator
- $\alpha_R \sim \omega_s$  so memory of integral only lasts a few synchrotron periods  
 $\Rightarrow \tau_t \cong r_t \cos(\omega_{st} n T_0 + \phi_t)$

$$V(t) = 2\alpha_R R_S I \int_{-\infty}^t e^{-\alpha_R(t-u)} \cos[\omega_R(r_t \cos(\omega_{st}t + \phi_t) - r_u \cos(\omega_{su}t + \phi_u))] + \omega_z(t-u)] du$$

The driving term is now analytically integrable, resulting in an infinite Fourier-Bessel series

$$V(t) = 2\alpha_R R_S I \operatorname{Re} \left\{ \sum_{p,m=-\infty}^{\infty} \frac{j^{p-m} J_p(r_t) J_m(r_u) e^{j(p\omega_{st} + m\omega_{su})t} e^{jp\phi_t + jm\phi_u}}{\alpha_r + j(m\omega_{su} - \omega_z)} \right\}$$

This is still a very complex expression, so we exploit the slowly varying character, w.r.t.  $\omega_s$ , of the amplitude,  $r_t$ , and phase,  $\phi_t$ , of the oscillation.

## 9.3 Krylov-Bogoliubov-Mitropolskii (KBM) Averaging Method

- Driven harmonic oscillator

$$\ddot{\tau} + \omega_{s_0}^2 \tau = f_{\tau}(\tau, \dot{\tau})$$

- Define  $r(t), \phi(t)$ , from modified version of homogeneous solutions

$$\tau = r(t) \cos(\omega_{s_0} t + \phi(t))$$

$$\dot{\tau} = -\omega_{s_0} r(t) \sin(\omega_{s_0} t + \phi(t))$$

- Solve the following equations

$$\frac{d\tau}{dt} = \dot{\tau}$$

$$\frac{d\dot{\tau}}{dt} = \ddot{\tau} = f_{\tau}(\tau, \dot{\tau}) - \omega_{s_0}^2 \tau$$

- Obtain differential equations for  $r(t), \phi(t)$

$$\dot{r} = -\frac{1}{\omega_{s_0}} \sin(\omega_{s_0} t + \phi) f(r, \phi)$$

$$\dot{\phi} = -\frac{1}{r\omega_{s_0}} \cos(\omega_{s_0} t + \phi) f(r, \phi)$$

- Average over one period (Fourier components)

$$\dot{\bar{r}} = -\frac{1}{2\pi} \int_{t-\frac{2\pi}{\omega_{s0}}}^t \sin(\omega_{s0}\tau + \phi) f(r, \phi) d\tau$$

$$\dot{\bar{\phi}} = -\frac{1}{2\pi r} \int_{t-\frac{2\pi}{\omega_{s0}}}^t \cos(\omega_{s0}\tau + \phi) f(r, \phi) d\tau$$

- Equations of motion include terms from wake, radiation damping, and pendulum equation

$$\dot{\bar{r}}_t = -\frac{1}{2\omega_{st}} F_{S1}(\bar{r}, \bar{\phi}) - \alpha_{rad} \bar{r}_t$$

$$\dot{\bar{\phi}}_t = -\frac{1}{2\bar{r}_t \omega_{st}} F_{C1}(\bar{r}, \bar{\phi}) - \frac{1}{16} \bar{r}_t^2 \omega_{st}$$

where  $F_{C1}(\bar{r}, \bar{\phi})$  and  $F_{S1}(\bar{r}, \bar{\phi})$  are the Fourier coefficients w.r.t.  $(\omega_{s0}\tau + \phi)$ .

For a two particle model, the wake, and therefore its Fourier coefficients, depend on the properties of both particles. These coefficients, for a system with a source particle  $(r_u, \phi_u)$  carrying current,  $I$ , acting on a test particle  $(r_t, \phi_t)$  with infinitesimal charge, are

$$F_{S1} = -A \sum_{k=1}^{\infty} J_k(r_u) [J_{k-1}(r_t) + J_{k+1}(r_t)] \\ \times [(a_k^- - a_k^+) \cos(k\Delta\phi) - (b_k^- - b_k^+) \sin(k\Delta\phi)] \\ F_{C1} = A 2b_0^+ J_0(r_u) J_1(r_t) + A \sum_{k=1}^{\infty} J_k(r_u) [J_{k-1}(r_t) - J_{k+1}(r_t)] \\ \times [(b_k^- - b_k^+) \cos(k\Delta\phi) + (a_k^- - a_k^+) \sin(k\Delta\phi)]$$

where  $A = 2I (\alpha_R R_S) \frac{\omega_{s0}^2}{V_{RF} |\cos \phi_s|}$ ,  $\Delta\phi = \phi_t - \phi_u$  and

$$a_k^{\pm} = \frac{\alpha_R}{\alpha_R^2 + (k\omega_{su} \pm \omega_z)^2}; \quad b_k^{\pm} = \frac{(k\omega_{su} \pm \omega_z)}{\alpha_R^2 + (k\omega_{su} \pm \omega_z)^2}$$

which are proportional to  $\text{Re}\{Z(k\omega_{su} \pm \omega_z)\}$  and  $\text{Im}\{Z(k\omega_{su} \pm \omega_z)\}$ , respectively.

## 9.4 Analysis

Although this is still an infinite sum, the sum depends on  $\bar{r}$  the oscillation amplitude of the particles. From our data, this limits at about  $\pi/2$ , so the series converges quickly. For our parameters, in fact, a very good understanding comes from keeping only the lowest terms. These forces have a strong dipole characteristic.

### 9.4.1 Linear theory

$(r_t, \phi_t) = (r_u, \phi_u)$  and use small amplitude expansion of  $J_n(r)$ .

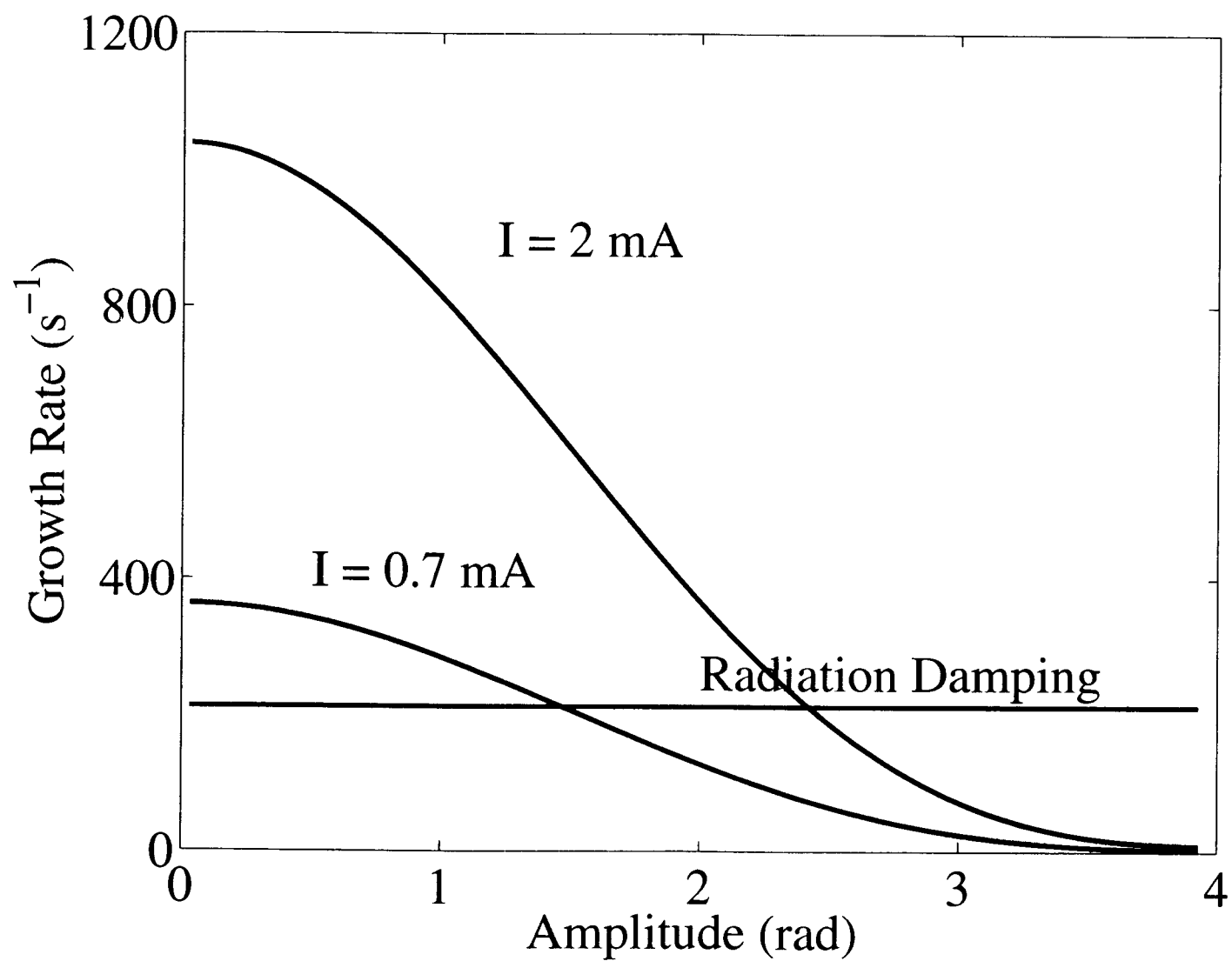
- Gives instability thresholds of linear theory
- Shows odd symmetry of growth/damping and frequency shift with respect to the fractional part of the resonator frequency,  $\omega_z$

### 9.4.2 Saturation

$(r_t, \phi_t) = (r_u, \phi_u)$  but now evaluate non-linearities in sum

- Decrease in amplitude of sum with increasing argument gives saturation mechanism
- Data shows saturation at earlier level, consistent with particle loss from main bunch

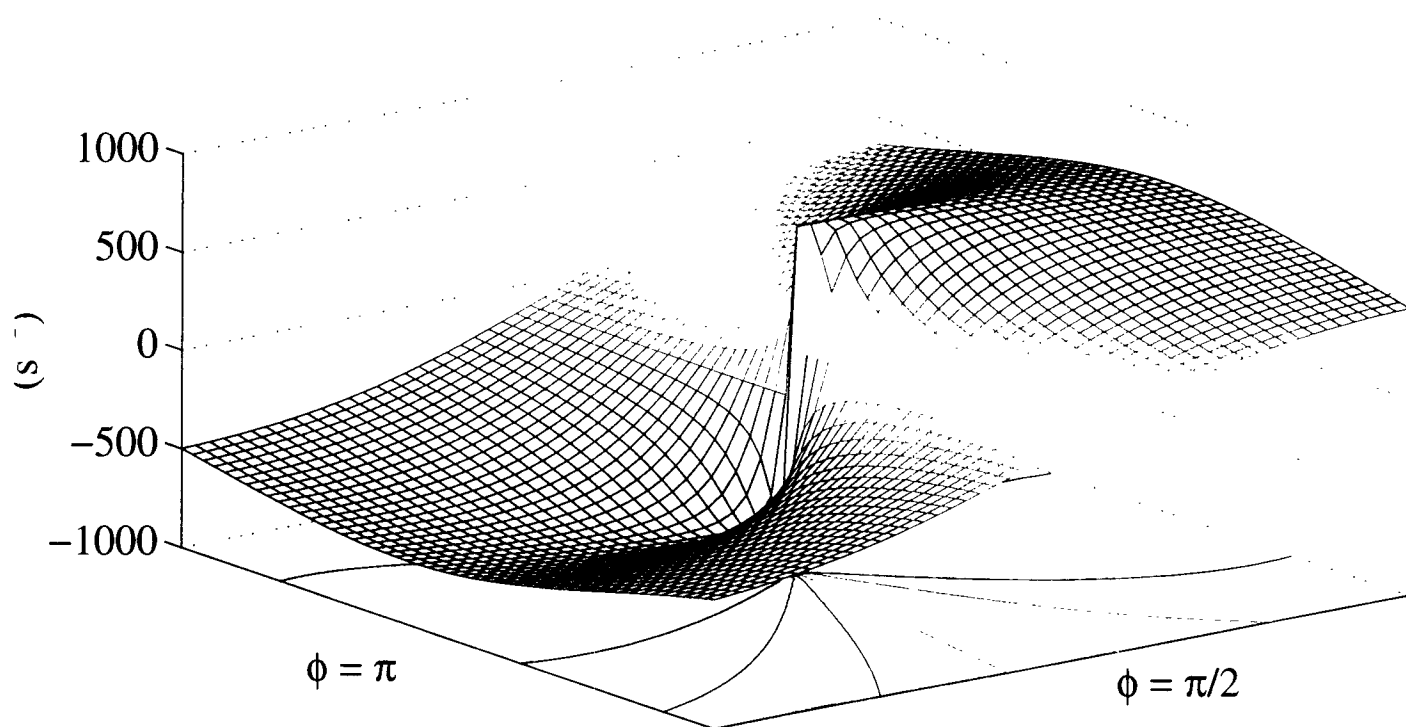




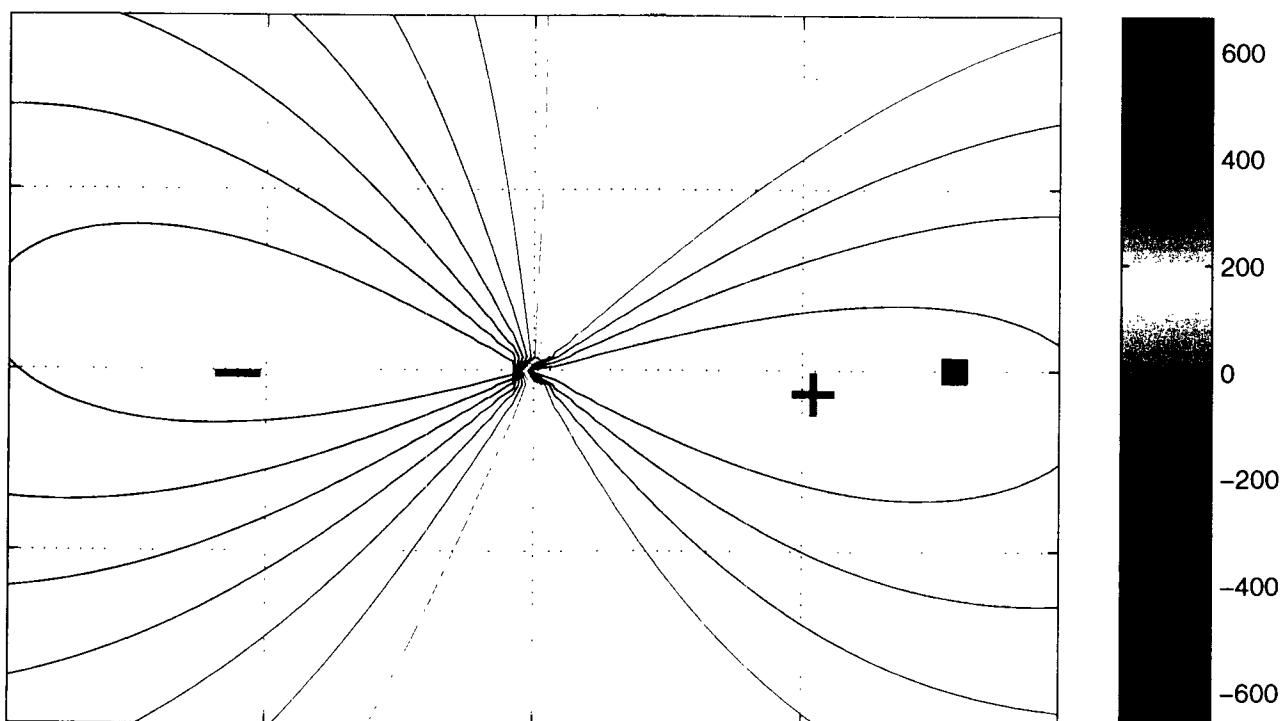
### 9.4.3 Diffusion

- To evaluate ‘stability’ of bunch as a macroparticle, look at situation of source particle,  $(r_u, \phi_u)$ , carrying all charge and examine behavior of test particle,  $(r_t, \phi_t)$ , at arbitrary location in phase space.
- Move to rotating coordinate frame in which  $\phi_u = 0$
- In this frame, consider if separation between  $(r_t, \phi_t)$  and  $(r_u, \phi_u)$  is increasing or decreasing
- At small amplitudes
  - $F_{S1} \Rightarrow$  radial restoring force
  - $F_{C1} \Rightarrow$  azimuthal restoring force
  - $\Rightarrow$  macroparticle is stable

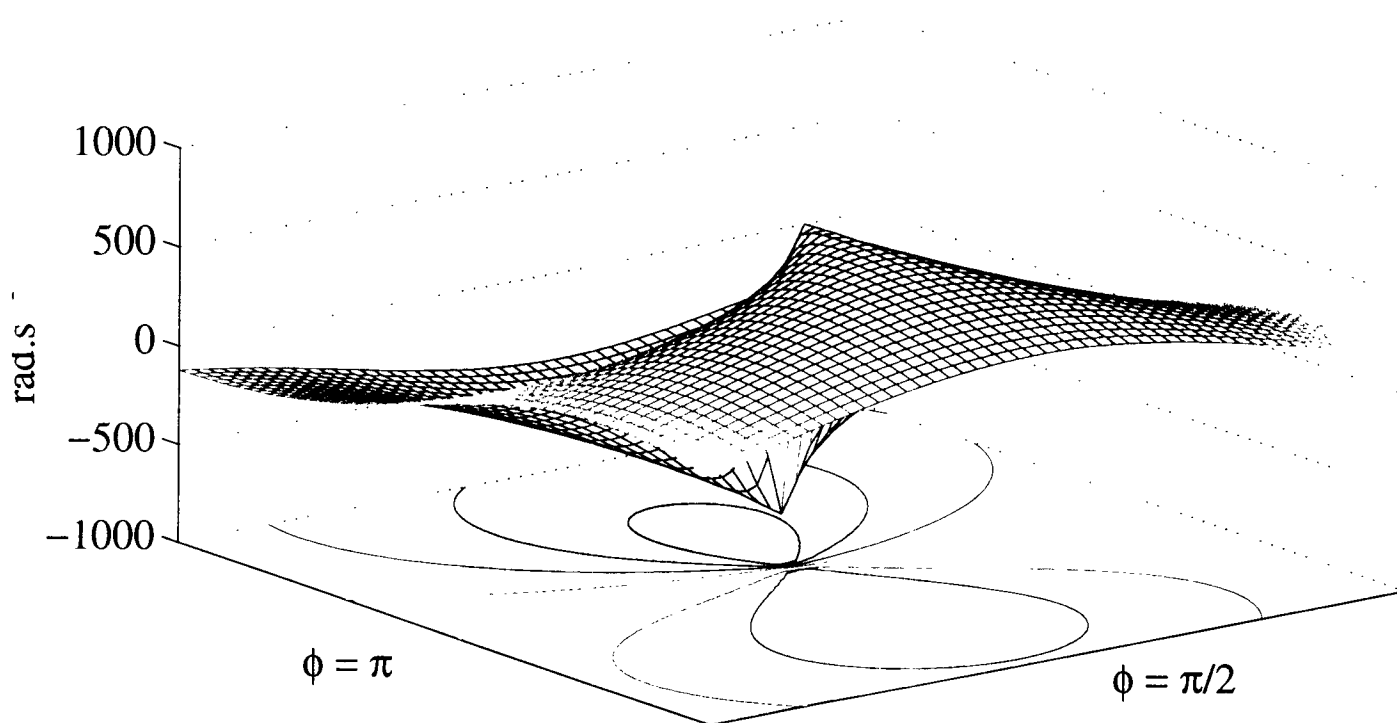
Growth from Wake



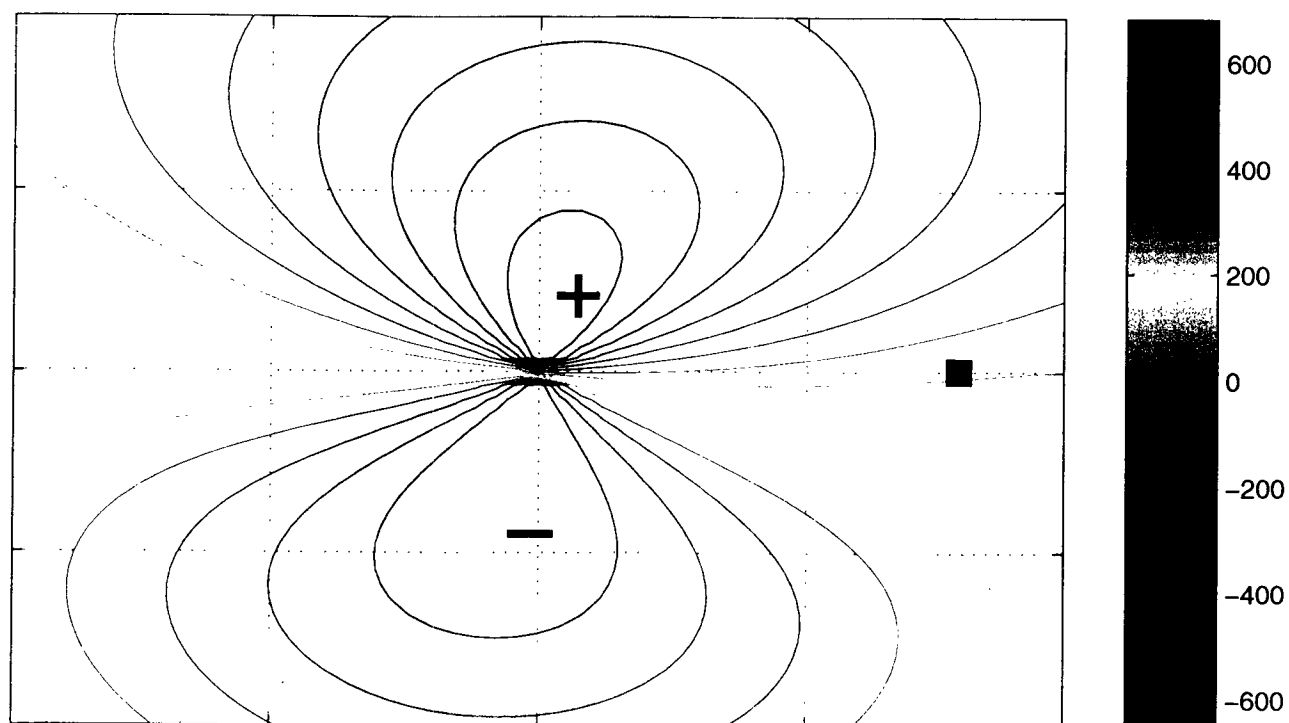
Main Body at  $\pi/4$

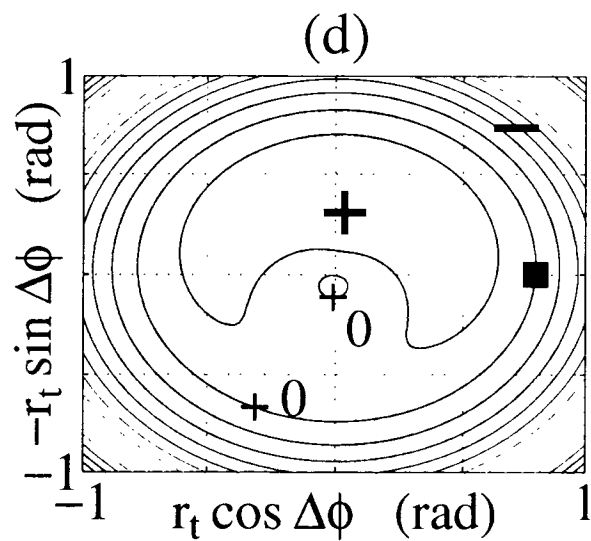
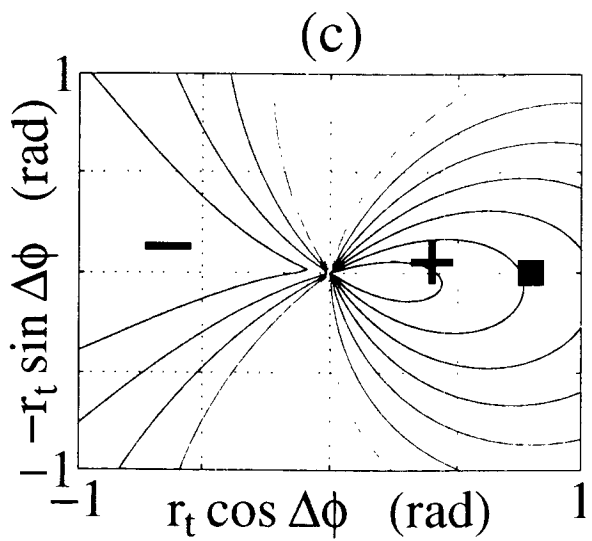
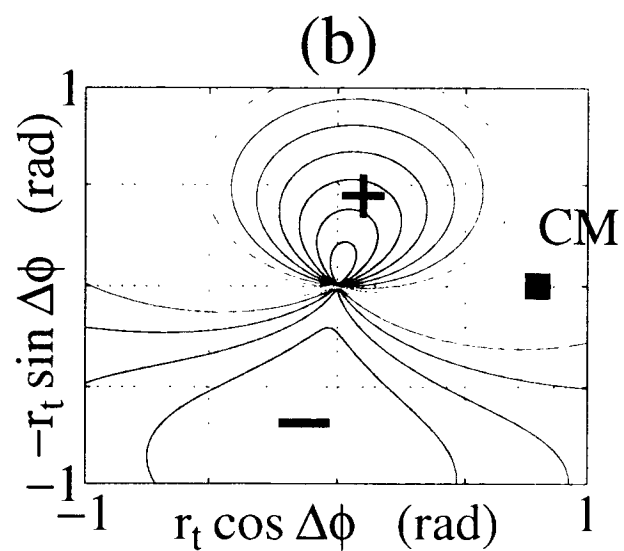
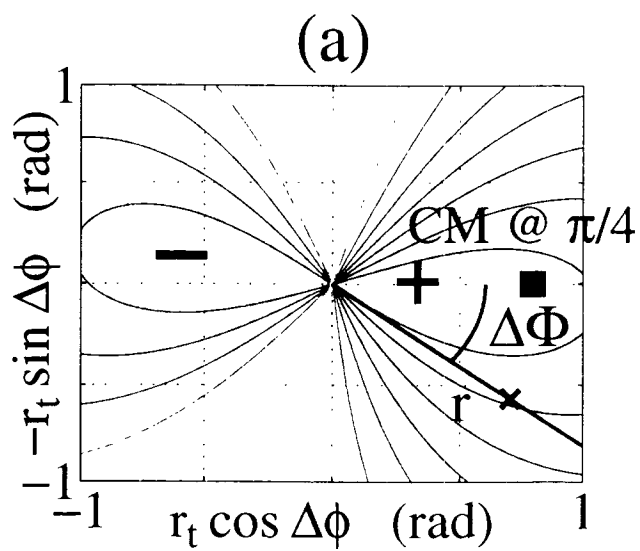


rd $\Phi$ /dt Frequency Shift from Wake



Main Body at  $\pi/4$





- At large amplitudes
  - Characteristics of radial forces are unchanged
  - Azimuthal force now dominated by pendulum effect
    - \* Test particle that falls behind macroparticle sees less  $\dot{\vec{r}}$ , drops toward the origin, gains  $\dot{\vec{\phi}}$ , and returns to region of larger  $\dot{\vec{r}}$ .
    - \* Test particle that moves ahead also sees less  $\dot{\vec{r}}$ , drops toward the origin, gains even more  $\dot{\vec{\phi}}$ , and exits macroparticle from the front.
  - As test particle rotates away from macroparticle, the net wake forces oscillate and lose their strength. Radiation damping brings the test particle back toward the origin.
  - Loss of charge from macroparticle also brings it closer to the origin

This change from attraction to the macroparticle to repulsion from it shows the change in dynamics of the system needed to form the second attractor and create the necessary conditions for the relaxation oscillation.

### 9.4.4 Location of second attractor near origin

When the macroparticle has a finite amplitude, a test particle at the origin still sees finite wake terms. Since the equation for  $\bar{\phi}$  has an additional  $r^{-1}$  factor multiplying the wake contribution,  $\bar{\phi}$  can assume any value near the origin. In particular, there exists a locus of points near the origin that are phase locked to the macroparticle. When the test particle reaches this locus, it again sees the wake of the macroparticle.

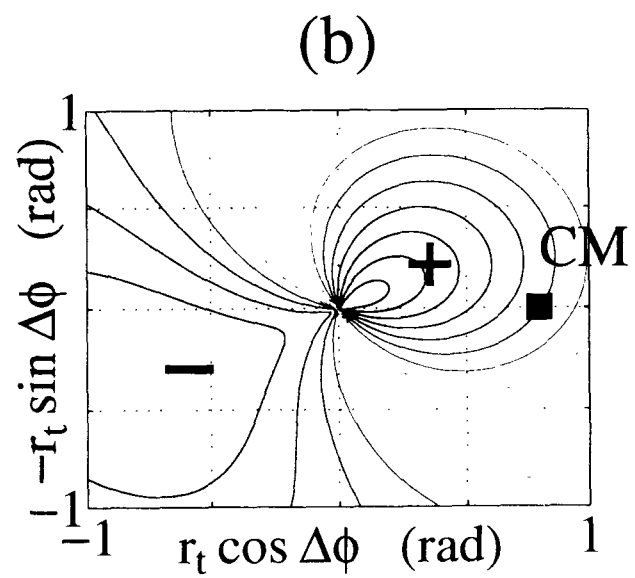
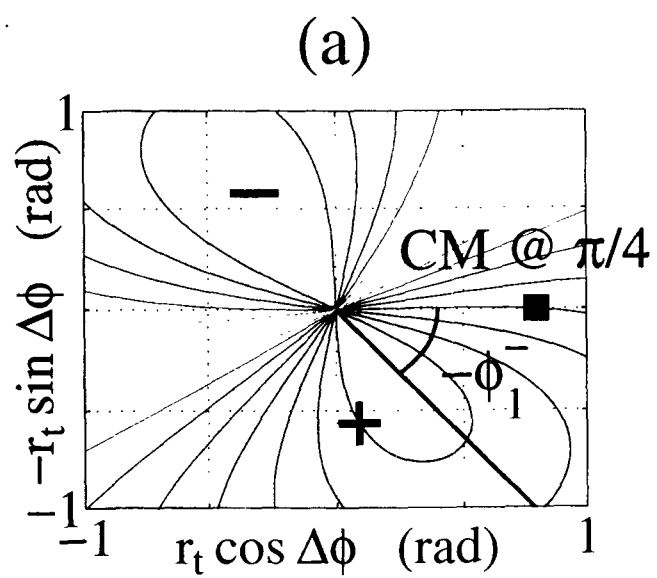
- Second attractor moves slowly  $\Rightarrow$  close to fixed point ( $\dot{r} = 0$ ) about  $\pi/2$  ahead of macroparticle
- As particles accumulate at this second attractor its charge increases
  - Contributes to its own growth
  - Azimuthal coordinate increases since it needs to see damping from original attractor
  - Amplitude grows
  - Two centers exert damping force on each other
  - Initial attractor damps

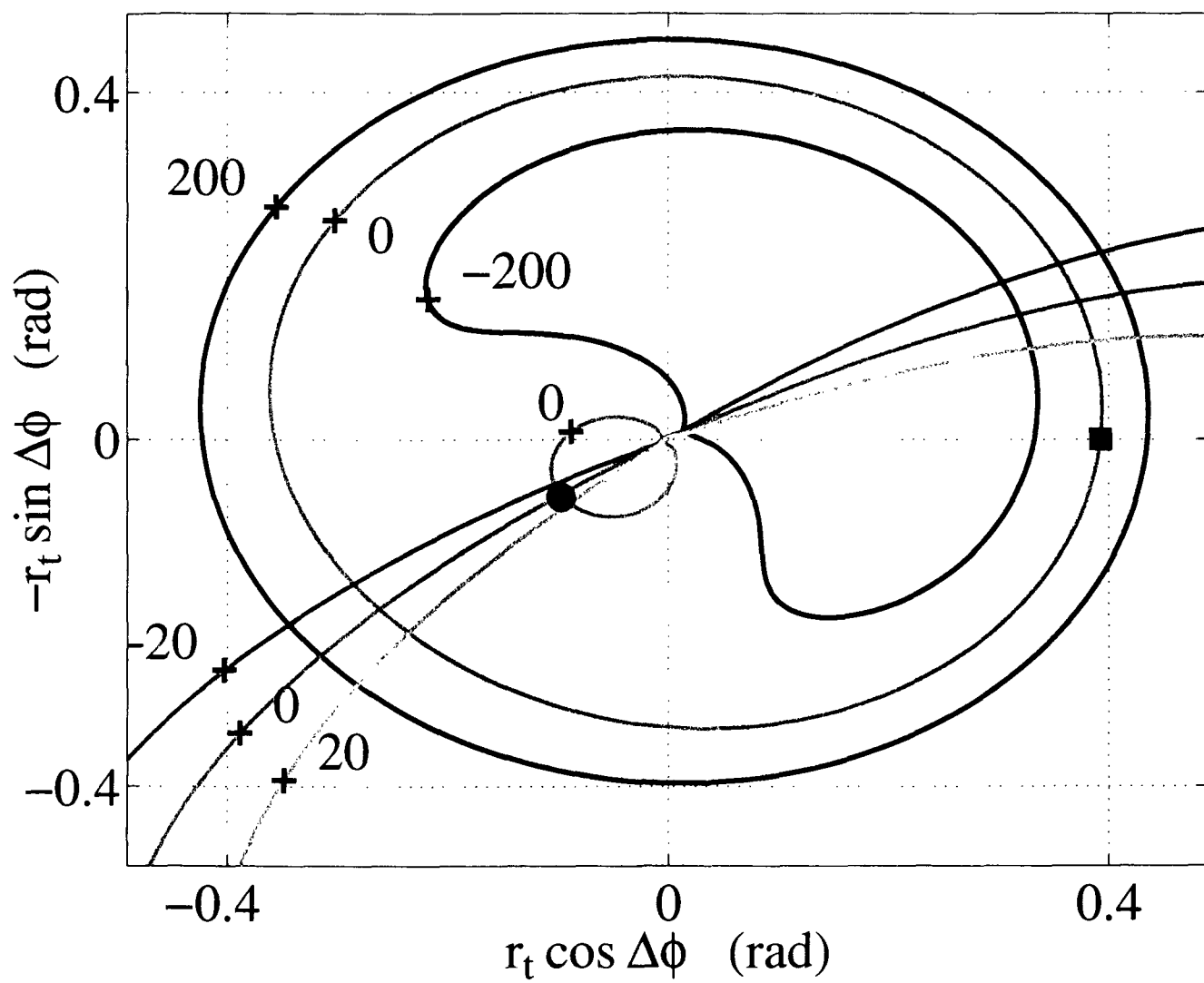
Relaxation cycle is then a flow of particles between two centers, with cycle frequency  $1/2$  that of observed signal.

### 9.4.5 Asymmetry of damping and observation of second attractor

- When  $\omega_z > \omega_s$ ,  $F_{S1}$  and  $F_{C1}$  rotate clockwise with two results
- Test particles pass through higher regions of  $F_{S1}$  as they try to escape from the front of the bunch  
 $\Rightarrow$  longer time needed for macroparticle to decay
- Node of shifted closer to  $\pi \Rightarrow$  second attractor close to  $\dot{r} = 0$  out of phase with initial attractor







# 10 Conclusions

- Experimental observations
  - Data gives complete characterization of phenomenon
- Simulations
  - Good agreement with experiments (low frequency behavior, ● lamentation)
  - Additional predictive power of direction of ● lamentation
- Analytic model
  - Exact derivation of long term wake potential
  - Theoretical explanation of phenomenon explains
    - \* Instability theory of linear model
    - \* Saturation mechanism of synchrotron oscillation
    - \* Diffusion mechanism
    - \* Conditions for relaxation oscillation
    - \* Creation and location of second attractor
    - \* Asymmetry of damping mechanism